Journal of Mechanics Engineering and Automation 4 (2014) 820-827

Determination of Natural Frequencies of Multilayered Plates by Mixed Finite Elements

Roberto S. Carnicer, Braian A. Desía and Rodolfo A. Schwarz

Faculty of Engineering, University of Belgrano, Autonomous City of Buenos Aires C1426BMJ, Argentina

Received: June 03, 2014 / Accepted: June 17, 2014 / Published: October 25, 2014.

Abstract: Natural frequencies for multilayer plates are calculated by mixed finite element method. The main object of this paper is to use the mixed model for multilayer plates, analyzing each layer as an isolated plate, where the continuity of displacements is achieved by Lagrange multipliers (representing static variables). This procedure allows us to work with any model for single plate (so as to ensure the proper behavior of each layer), and the complexity of the multilayer system is avoided by ensuring the condition of displacements by the Lagrange multipliers (static variables). The plate is discretized by finite element modeling based on a primary hybrid model, where the domain is divided by quadrilateral, both for the displacement field and static variables. This mixed element for plates was implemented and several examples of vibrations have been verified successfully by the results obtained by other methods in the literature.

Key words: Mixed finite element, multilayer plate, Lagrange multipliers, natural frequencies, free vibrations.

1. Introduction

Advanced composite materials are widely used in many specialties of engineering such as civil engineering, naval engineering and aerospace engineering due to its high strength to weight ratio, excellent corrosion resistance, good fatigue behavior and other superior properties compared to conventional materials. A detailed analysis of the advantages of these materials is given by Jones [1].

Among the different types of composite materials, laminates are the most popular due to their variety of structural applications in situations where high and flexural membrane strength is required. The composite laminates are basically plates formed of several layers which are perfectly linked together, presenting an anisotropic behavior. Each layer is comprised of fibers embedded in a matrix. These fibers confer higher mechanical properties to the laminate in the direction of the fiber, while the matrix keeps them linked. The layers are placed one over other oriented according to the design requirements in order to optimize the use of material.

The anisotropy of the composite materials leads to a complicated mechanical behavior which differs from the traditional materials. Its growing employment requires the development of efficient and accurate numerical methods to adequately predict its complex behavior.

In this paper, a solution based on a layered model for the determination of modal characteristics from finite elements with mixed variables (kinematic and static) is proposed. The paper is organized as follows: Section 2 presents the mathematical formulation of the problem; Section 3 develops the finite element model, obtaining the governing equations by means of the Hamilton's principle; Section 4 shows a methodology to solve the eigenproblem based on the inverse iterative vector method; Several examples are solved and exposed in Section 5; Finally, Section 6 presents the conclusions.

Corresponding author: Carnicer S. Roberto, professor, research fields: finite elements, structural engineering. E-mail: rcarnicer@freyreyasoc.com.ar.

2. Problem Formulation

A plate composed of "n" layers of height "h" is considered. And a system of local Cartesian coordinates (x, y, z) for each layer in the middle surface Ω_i is defined. where x, y are the in plane coordinates and z is the normal coordinate. The upper face is located at $z = -h_i/2$, and the bottom at $z = +h_i/2$.

Each layer is modeled independently, adopting the Reissner-Mindlin shear deformation theory (FSDT). Thus, the displacement field for a point (x, y, z) of a generic layer "i" is given by:

$$\begin{aligned} u_{xi} &= u_{oxi}(x,y) - z_i\ \beta_{xi}(x,y) \\ u_{yi} &= u_{oyi}(x,y) - z_i\ \beta_{yi}(x,y) \\ w_i &= w_{oi}(x,y) \end{aligned} \tag{1}$$

where, $\underline{\mathbf{u}}_i = [u_{oxi},\ u_{oyi}]^{\mathrm{T}}$ are displacements in the midplane, w_i is the vertical displacement (assumed constant throughout the thickness considering the normal to midplane inextensible) and $\underline{\boldsymbol{\beta}}_i = [\beta_{xi},\ \beta_{yi}]^{\mathrm{T}}$ are normal cross rotations about axes y, x, respectively.

The functional of the Reissner-Mindlin potential energy for a generic layer "i", in function ($\underline{u}_i$, $\underline{\beta}_i$, w_i) is expressed as:

$$\begin{aligned} \Pi_i\left(\underline{u}_i, \underline{\beta}_i, w_i\right) = &\frac{1}{2} h_i\, a\left(\underline{u}_i, \underline{u}_i\right) \\ &+ \frac{1}{2}\frac{h_i^3}{12} a\left(\underline{\beta}_i, \underline{\beta}_i\right) \\ &+ \frac{1}{2} h_i\, b\left(\underline{\nabla} w_i - \underline{\beta}_i - \underline{\nabla} w_i - \underline{\beta}_i\right) \end{aligned} \tag{2}$$

where, the bilinear operators $a(\underline{u}_i,\ \underline{u}_i)$ and $a(\underline{\beta}_i,\ \underline{\beta}_i)$ represent the membranal and flexural deformation energy, respectively; while $b(\underline{\nabla} w_i - \underline{\beta}_i, (\underline{\nabla} w_i - \underline{\beta}_i)$ is the shear energy deformation. In the analysis of free vibrations, the potential energy due to external work of the applied loads is zero.

Meanwhile, the functional of the kinetic energy for a generic layer in terms of ($\underline{u}_i$, $\underline{\beta}_i$, w_i) is expressed as:

$$\begin{aligned} \mathrm{T}_i\left(\dot{\underline{u}}_i, \dot{\underline{\beta}}_i, \dot{w}_i\right) = &\frac{1}{2} h_i\, c\left(\dot{\underline{u}}_i, \dot{\underline{u}}_i\right) \\ &+ \frac{1}{2}\frac{h_i^3}{12} c\left(\dot{\underline{\beta}}_i, \dot{\underline{\beta}}_i\right) + \frac{1}{2} h_i\, c\left(\dot{w}_i, \dot{w}_i\right) \end{aligned} \tag{3}$$

where, $c(\dot{\underline{u}}_i,\ \dot{\underline{u}}_i)$, $c(\dot{\underline{\beta}}_i,\ \dot{\underline{\beta}}_i)$ and $c(\dot{w}_i,\ \dot{w}_i)$represent the kinetic energy operators related to the plane, rotational and transverse inertia, respectively. The time derivative is indicated by a dot.

The behavior of the layers that make up the system requires the continuity of displacements between adjacent layers (Fig. 1), for which the following kinematic constraints are imposed:

(1) Displacements $u_{oxi}(x, y, h_i/2)$ and $u_{oyi}(x, y, h_i/2)$ in the interface $i + 1$,

$$\begin{aligned} u_{xi}\left(x, y, -\frac{h_i}{2}\right) &= u_{oxi}(x,y) - \frac{h_i}{2}\beta_{xi}(x,y) \\ u_{yi}\left(x, y, \frac{h_i}{2}\right) &= u_{oyi}(x,y) - \frac{h_i}{2}\beta_{yi}(x,y) \end{aligned} \tag{4}$$

should be equal to the displacements $u_{oxi+1}(x, y, -h_{i+1}/2)$ and $u_{oyi+1}(x, y, -h_{i+1}/2)$ in the interface $i + 1$,

$$\begin{aligned} u_{xi+1}\left(x, y, -\frac{h_{i+1}}{2}\right) &= u_{oxi+1}(x,y) + \frac{h_{i+1}}{2}\beta_{xi+1}(x,y) \\ u_{yi+1}\left(x, y, -\frac{h_{i+1}}{2}\right) &= u_{oyi+1}(x,y) + \frac{h_{i+1}}{2}\beta_{yi+1}(x,y) \end{aligned} \tag{5}$$

so

$$\begin{aligned} u_{xi}\left(x, y, h_i/2\right) &= u_{xi+1}\left(x, y, -h_{i+1}/2\right) \\ u_{yi}\left(x, y, h_i/2\right) &= u_{yi+1}\left(x, y, -h_{i+1}/2\right) \end{aligned} \tag{6}$$

(2) Vertical displacements w_i for layer "i" should be the same that the vertical displacements w_{i+1} for layer $i + 1$:

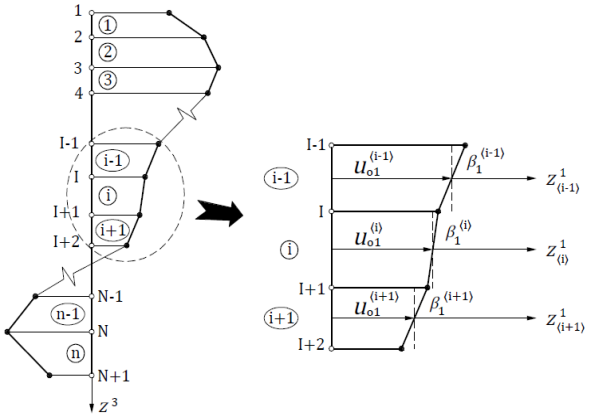

Fig. 1 Displacements fields along height for the layer-wise model.

$$w_i(x,y) = w_{i+1}(x,y) \tag{7}$$

Thus, the multilayer system is obtained as a superposition of "*n*" simple plates, where the requirements of kinematic continuity are ensured mathematically from the inclusion of Lagrange multipliers $\underline{\boldsymbol{\lambda}}_j = [\lambda_{xj},\ \lambda_{yj}]^{\mathrm{T}}$ and μ_j represents interlaminar stresses (surface forces) at the interface "*j*". In this way, the functional of the total potential energy of the system is defined as:

$$\begin{aligned}\Pi_i\left(\underline{u}_i,\underline{\beta}_i,w_i,\underline{\lambda}_i,\mu_i\right) = \sum_{i=1}^{n}\Bigg\{&\frac{1}{2}h_i\,a\left(\underline{u}_i,\underline{u}_i\right)\\ &+\frac{1}{2}\frac{h_i^3}{12}a\left(\underline{\beta}_i,\underline{\beta}_i\right)\\ &+\frac{1}{2}h_i\,b\left(\underline{\nabla}w_i-\underline{\beta}_i-\underline{\nabla}w_i-\underline{\beta}_i\right)\Bigg\}\\ +\sum_{j=1}^{n-1}\Bigg\{&\iint_{\Omega_{j+1}}\Bigg[\left(u_j-\beta_j\frac{h_j}{2}\right)\\ &-\left(u_{j+1}-\beta_{j+1}\frac{h_{j+1}}{2}\right)\Bigg]\lambda_{j+1}\,\mathrm{d}\Omega\\ &+\iint_{\Omega_{j+1}}\left[\left(w_j-w_{j+1}\right)\mu_{j+1}\,\mathrm{d}\Omega\right]\Bigg\}\end{aligned} \tag{8}$$

While the functional of the total kinetic energy is demonstrated by:

$$\begin{aligned}\mathrm{T}_i\left(\dot{\underline{u}}_i,\dot{\underline{\beta}}_i,\dot{w}_i\right) = \sum_{i=1}^{n}\Bigg\{&\frac{1}{2}h_i\,c\left(\dot{\underline{u}}_i,\dot{\underline{u}}_i\right)\\ &+\frac{1}{2}\frac{h_i^3}{12}c\left(\dot{\underline{\beta}}_i,\dot{\underline{\beta}}_i\right)+\frac{1}{2}h_i\,c\left(\dot{w}_i,\dot{w}_i\right)\Bigg\}\end{aligned} \tag{9}$$

The justification of the physical meaning of the Lagrange multipliers is obtained by Alliney and Carnicer [2].

3. Finite Elements Discretization

The equations governing the problem are achieved by the Hamilton's principle.

$$\delta\int_{t1}^{t2}(\Pi-\mathrm{T})\,\mathrm{d}t = 0 \tag{10}$$

Introducing Eqs. (8) and (9) into Eq. (10), and taking the variation, the Euler-Lagrange expressions of the variational problem are obtained.

$$\begin{aligned}&h_i\,a(\underline{u}_i,\delta\underline{u}_i)+\int_{\Omega_i}\underline{\lambda}_i\,\delta\underline{u}_i\,\mathrm{d}\Omega\\ &\int_{\Omega_{i+1}}\underline{\lambda}_{i+1}\,\delta\underline{u}_i\,\mathrm{d}\Omega-h_i\,c(\dot{\underline{u}}_i,\delta\dot{\underline{u}}_i)=0\end{aligned} \tag{11}$$

$$\begin{aligned}&\frac{h_i^3}{12}a(\underline{\beta}_i,\delta\underline{\beta}_i)+h_i\,b(\underline{\nabla}w_i-\underline{\beta}_i,-\delta\underline{\beta}_i)\\ &-\int_{\Omega_i}\frac{h_i}{12}\underline{\lambda}_i\,\delta\underline{\beta}_i\,\mathrm{d}\Omega+\int_{\Omega_{i+1}}\frac{h_i}{12}\underline{\lambda}_{i+1}\,\delta\underline{\beta}_i\,\mathrm{d}\Omega\\ &-\frac{h_i^3}{12}c(\dot{\underline{\beta}}_i,\delta\dot{\underline{\beta}}_i)=0\end{aligned} \tag{12}$$

$$\begin{aligned}&h_i\,b(\underline{\nabla}w_i-\underline{\beta}_i,\delta\underline{\nabla}w_i)-\int_{\Omega_i}\mu_i\,\delta w_i\,\mathrm{d}\Omega\\ &\int_{\Omega_{i+1}}\lambda_{i+1}\,\delta w_i\,\mathrm{d}\Omega-h_i\,c(\dot{w}_i,\delta\dot{w}_i)=0\end{aligned} \tag{13}$$

$$\int_{\Omega_i}\left[\left(\underline{u}_{i-1}-\underline{\beta}_{i-1}\frac{h_{i-1}}{2}\right)-\left(\underline{u}_i-\underline{\beta}_i\frac{h_i}{2}\right)\right]\delta\underline{\lambda}_i\,\mathrm{d}\Omega=0 \tag{14}$$

$$\delta\int_{\Omega_i}\left(w_{i-1}-w_{\mathrm{i}}\right)\delta\mu_{\mathrm{i}}\,\mathrm{d}\Omega=0 \tag{15}$$

The set of equations obtained contains first derivatives of the dependent variables ($\underline{u}_i$, $\underline{\beta}_i$, w_i), so that the shape functions thereof require C^0 continuity, while for the dependent variables ($\underline{\lambda}_j$, μ_i) supported continuity C^{-1} to not show their derivatives. Likewise, for simplicity, the same interpolation for all variables is adopted [3].

$$\left(\underline{u}_i,\underline{\beta}_i,w_i,\underline{\lambda}_j,\mu_i\right)=\sum_{q=1}^{NN}N_q\left(\underline{u}_i^q,\underline{\beta}_i^q,w_i^q,\underline{\lambda}_j^q,\mu_j^q\right) \tag{16}$$

where, *NN* is the number of nodes by element and N_q are the interpolation functions associated to node "*q*". Replacing Eq. (16) into Eqs. (11)-(15), the finite element model is defined as follows:

$$\begin{aligned}&\delta\underline{u}_i^{\mathrm{T}}\cdot\Big[\underline{\mathrm{A}}_i^m\cdot\underline{u}_i-\underline{\mathrm{B}}_i^{\langle i\rangle}\cdot\underline{\lambda}_i+\underline{\mathrm{B}}_i^{\langle i+1\rangle}\cdot\underline{\lambda}_{i+1}\\ &-\underline{m}_i^{ip}\cdot\ddot{\underline{u}}_i\Big]=0\end{aligned} \tag{17}$$

$$\begin{aligned}&\delta\underline{\beta}_i^{\mathrm{T}}\cdot\Big[\underline{\mathrm{A}}_i^b\cdot\underline{\beta}_i-\underline{E}_i\cdot\underline{w}_i+\underline{D}_i\cdot\underline{\beta}_i\\ &-\underline{\mathrm{C}}_i^{\langle i\rangle}\cdot\underline{\lambda}_i-\underline{\mathrm{C}}_i^{\langle i+1\rangle}\cdot\underline{\lambda}_{i+1}-\underline{m}_i^r\cdot\ddot{\underline{\beta}}_i=0\end{aligned} \tag{18}$$

$$\begin{aligned}&\delta\underline{w}_i^{\mathrm{T}}\cdot\Big[\underline{\mathrm{G}}_i\cdot\underline{w}_i-\underline{\mathrm{E}}_i^{\mathrm{T}}\cdot\underline{\beta}_i-\underline{\mathrm{H}}_i^{\langle i\rangle}\cdot\underline{\mu}_i\\ &+\underline{\mathrm{H}}_i^{\langle i+1\rangle}\cdot\underline{\mu}_{i+1}-\underline{m}_i^{op}\cdot\ddot{\underline{w}}_i\Big]=0\end{aligned} \tag{19}$$

$$\begin{aligned}&\delta\underline{\lambda}_j^{\mathrm{T}}\cdot\Big[\underline{\mathrm{B}}_{j-1}^{\langle j\rangle\mathrm{T}}\cdot\underline{u}_{j-1}-\underline{\mathrm{C}}_{j-1}^{\langle j\rangle\mathrm{T}}\cdot\underline{\beta}_{j-1}\\ &+\underline{\mathrm{B}}_j^{\langle j\rangle\mathrm{T}}\cdot\underline{u}_j-\underline{\mathrm{C}}_j^{\langle j\rangle\mathrm{T}}\cdot\underline{\beta}_j\Big]=0\end{aligned} \tag{20}$$

$$\delta \underline{\mu}_j^{\mathrm{T}} \cdot \left[\underline{\mathrm{H}}_{j-1}^{\langle j \rangle \mathrm{T}} \cdot \underline{w}_{j-1} - \underline{\mathrm{H}}_j^{\langle j \rangle \mathrm{T}} \cdot \underline{w}_j \right] = 0 \qquad (21)$$

For a system of three layers, the matrix compact representation is:

$$\begin{vmatrix} \underline{\mathrm{C}}_{11} & \underline{\mathrm{Q}}_{12}^{\mathrm{T}} & & & \\ \underline{\mathrm{Q}}_{12} & \underline{0} & \underline{\mathrm{Q}}_{22}^{\mathrm{T}} & \underline{0} & \\ & \underline{\mathrm{Q}}_{22} & \underline{\mathrm{C}}_{22} & \underline{\mathrm{Q}}_{23}^{\mathrm{T}} & \\ & & \underline{\mathrm{Q}}_{12} & \underline{0} & \underline{\mathrm{Q}}_{33}^{\mathrm{T}} \\ & & & \underline{\mathrm{Q}}_{33} & \underline{\mathrm{C}}_{33} \end{vmatrix} \cdot \begin{vmatrix} \underline{\mathrm{x}}_1 \\ \underline{\lambda}_2 \\ \underline{\mathrm{x}}_2 \\ \underline{\lambda}_3 \\ \underline{\mathrm{x}}_3 \end{vmatrix} =$$

$$= \begin{vmatrix} \underline{\mathrm{M}}_{11} & \underline{0} & & & \\ \underline{0} & \underline{0} & \underline{0} & \underline{0} & \\ & \underline{0} & \underline{\mathrm{M}}_{22} & \underline{0} & \\ & \underline{0} & \underline{0} & \underline{0} & \underline{0} \\ & & & \underline{0} & \underline{\mathrm{M}}_{33} \end{vmatrix} \cdot \begin{vmatrix} \ddot{\underline{\mathrm{x}}}_1 \\ \underline{\lambda}_2 \\ \ddot{\underline{\mathrm{x}}}_2 \\ \underline{\lambda}_3 \\ \ddot{\underline{\mathrm{x}}}_3 \end{vmatrix} \qquad (22)$$

where, $\underline{\mathbf{x}}_i = [\underline{u}_i, \underline{\beta}_i, \underline{w}_i]^{\mathrm{T}}$ are kinematic variables, $\underline{\boldsymbol{\lambda}}_i = [\underline{\lambda}_i, \underline{\mu}_i]^{\mathrm{T}}$ are static variables, ($\underline{C}_{ii}$, $\underline{M}_{ii}$) are the stiffness and mass contributions each layer, respectively, and ($\underline{\mathbf{Q}}_{ii}$, $\underline{\mathbf{Q}}_{ij}$) are the Lagrange restriction matrix results.

In free vibrations without damping analysis, the response of the plate is assumed periodic.

$$\underline{x}_i = \underline{x}_i^o \, e^{\mathrm{i}\, w\, t} \qquad (23)$$

where, $\underline{x}_i^{\mathrm{o}}$ is the independent of time amplitude and ω is the vibration angular frequency of the system. Replacing Eq. (23) into Eq. (22), the eingenploblem is given in Eq. (24).

$$\begin{vmatrix} \underline{\mathrm{C}}_{11} & \underline{\mathrm{Q}}_{12}^{\mathrm{T}} & & & \\ \underline{\mathrm{Q}}_{12} & \underline{0} & \underline{\mathrm{Q}}_{22}^{\mathrm{T}} & \underline{0} & \\ & \underline{\mathrm{Q}}_{22} & \underline{\mathrm{C}}_{22} & \underline{\mathrm{Q}}_{23}^{\mathrm{T}} & \\ & & \underline{\mathrm{Q}}_{12} & \underline{0} & \underline{\mathrm{Q}}_{33}^{\mathrm{T}} \\ & & & \underline{\mathrm{Q}}_{33} & \underline{\mathrm{C}}_{33} \end{vmatrix} \cdot \begin{vmatrix} \underline{\mathrm{x}}_1^{\mathrm{o}} \\ \underline{\lambda}_2 \\ \underline{\mathrm{x}}_2^{\mathrm{o}} \\ \underline{\lambda}_3 \\ \underline{\mathrm{x}}_3^{\mathrm{o}} \end{vmatrix} =$$

$$= \omega^2 \begin{vmatrix} \underline{\mathrm{M}}_{11} & \underline{0} & & & \\ \underline{0} & \underline{0} & \underline{0} & \underline{0} & \\ & \underline{0} & \underline{\mathrm{M}}_{22} & \underline{0} & \\ & \underline{0} & \underline{0} & \underline{0} & \underline{0} \\ & & & \underline{0} & \underline{\mathrm{M}}_{33} \end{vmatrix} \cdot \begin{vmatrix} \underline{\mathrm{x}}_1^{\mathrm{o}} \\ \underline{\lambda}_2 \\ \underline{\mathrm{x}}_2^{\mathrm{o}} \\ \underline{\lambda}_3 \\ \underline{\mathrm{x}}_3^{\mathrm{o}} \end{vmatrix} \qquad (24)$$

The non-trivial solution requires that,

$$\det\left(\underline{K} - \omega^2 \ \underline{M} \right) = 0 \qquad (25)$$

after imposed the boundary conditions.

4. Solving the Eigenproblem

As is characteristic of mixed formulation, the stiffness matrix generated is not positive definite, and neither is the mass matrix. Furthermore, the number of unknowns increases rapidly as more layers are added, so that the determination of the eigenvalue problem is difficult. In this section, a simple methodology for solving the problem based on the inverse iteration method [4] is proposed.

The procedure consists in initially establishing a test vector. Subsequently, the right hand of Eq. (24) is evaluated. Since eingenvectors can only be determined within a scale factor, choosing of ω^2 does not affect the result which it is assumed $\omega^2 = 1$. Thus, the vector of equivalent load is obtained.

$$\begin{vmatrix} \underline{\mathrm{M}}_{11} & \underline{0} & & & \\ \underline{0} & \underline{0} & \underline{0} & \underline{0} & \\ & \underline{0} & \underline{\mathrm{M}}_{22} & \underline{0} & \\ & \underline{0} & \underline{0} & \underline{0} & \underline{0} \\ & & & \underline{0} & \underline{\mathrm{M}}_{33} \end{vmatrix} \cdot \begin{vmatrix} \underline{\mathrm{x}}_{1,k} \\ \underline{\lambda}_{2,k} \\ \underline{\mathrm{x}}_{2,k} \\ \underline{\lambda}_{3,k} \\ \underline{\mathrm{x}}_{3,k} \end{vmatrix} = \begin{vmatrix} \underline{\mathrm{M}}_{11} \cdot \underline{\mathrm{x}}_{1,k} \\ \underline{0} \\ \underline{\mathrm{M}}_{22} \cdot \underline{\mathrm{x}}_{2,k} \\ \underline{0} \\ \underline{\mathrm{M}}_{33} \cdot \underline{\mathrm{x}}_{3,k} \end{vmatrix} \qquad (26)$$

Since initial vector is arbitrarily set, generally represented in Eq. (24) equality is not satisfied (if is fulfilled, the test vector is an eingenvector), so the following system of equations must be solved.

$$\begin{vmatrix} \underline{\mathrm{C}}_{11} & \underline{\mathrm{Q}}_{12}^{\mathrm{T}} & & & \\ \underline{\mathrm{Q}}_{12} & \underline{0} & \underline{\mathrm{Q}}_{22}^{\mathrm{T}} & \underline{0} & \\ & \underline{\mathrm{Q}}_{22} & \underline{\mathrm{C}}_{22} & \underline{\mathrm{Q}}_{23}^{\mathrm{T}} & \\ & & \underline{\mathrm{Q}}_{12} & \underline{0} & \underline{\mathrm{Q}}_{33}^{\mathrm{T}} \\ & & & \underline{\mathrm{Q}}_{33} & \underline{\mathrm{C}}_{33} \end{vmatrix} \cdot \begin{vmatrix} \underline{\mathrm{x}}_{1,k+1} \\ \underline{\lambda}_{2,k+1} \\ \underline{\mathrm{x}}_{2,k+1} \\ \underline{\lambda}_{3,k+1} \\ \underline{\mathrm{x}}_{3,k+1} \end{vmatrix} =$$

$$= \begin{vmatrix} \underline{\mathrm{M}}_{11} \cdot \underline{\mathrm{x}}_{1,k} \\ \underline{0} \\ \underline{\mathrm{M}}_{22} \cdot \underline{\mathrm{x}}_{2,k} \\ \underline{0} \\ \underline{\mathrm{M}}_{33} \cdot \underline{\mathrm{x}}_{3,k} \end{vmatrix} \qquad (27)$$

From Eq. (27), it results:

$$\begin{aligned}
\underline{\mathbf{C}}_{11}\cdot\underline{x}_{1,k+1} &= \underline{\mathbf{M}}_{11}\cdot\underline{x}_{1,k} - \underline{\mathbf{Q}}_{12}{}^{\mathrm{T}}\cdot\underline{\lambda}_{2,k+1} \\
\underline{\mathbf{C}}_{22}\cdot\underline{x}_{2,k+1} &= \underline{\mathbf{M}}_{22}\cdot\underline{x}_{2,k} - \underline{\mathbf{Q}}_{22}{}^{\mathrm{T}}\cdot\underline{\lambda}_{2,k+1} \\
&\quad - \underline{\mathbf{Q}}_{23}{}^{\mathrm{T}}\cdot\underline{\lambda}_{3,k+1} \\
\underline{\mathbf{C}}_{33}\cdot\underline{x}_{3,k+1} &= \underline{\mathbf{M}}_{33}\cdot\underline{x}_{3,k} - \underline{\mathbf{Q}}_{33}{}^{\mathrm{T}}\cdot\underline{\lambda}_{3,k+1}
\end{aligned} \tag{28}$$

Replacing the displacements on the remaining equations, the reduced matrix shown in Eq. (29) is obtained.

$$\begin{vmatrix}
\underline{\mathbf{Q}}_{12}\cdot\underline{\mathbf{C}}_{11}^{-1}\cdot\underline{\mathbf{Q}}_{12}^{\mathrm{T}} + \underline{\mathbf{Q}}_{22}^{\mathrm{T}}\cdot\underline{\mathbf{C}}_{22}^{-1}\cdot\underline{\mathbf{Q}}_{22} & \underline{\mathbf{Q}}_{22}^{\mathrm{T}}\cdot\underline{\mathbf{C}}_{22}^{-1}\cdot\underline{\mathbf{Q}}_{23}^{\mathrm{T}} \\
\underline{\mathbf{Q}}_{23}\cdot\underline{\mathbf{C}}_{22}^{-1}\cdot\underline{\mathbf{Q}}_{22} & \underline{\mathbf{Q}}_{23}\cdot\underline{\mathbf{C}}_{22}^{-1}\cdot\underline{\mathbf{Q}}_{23}^{\mathrm{T}} + \underline{\mathbf{Q}}_{33}^{\mathrm{T}}\cdot\underline{\mathbf{C}}_{33}^{-1}\cdot\underline{\mathbf{Q}}_{33}
\end{vmatrix} \cdot \begin{vmatrix} \underline{\lambda}_{2,k+1} \\ \underline{\lambda}_{3,k+1} \end{vmatrix} =$$

$$= \begin{vmatrix}
\underline{\mathbf{Q}}_{12}\cdot\underline{\mathbf{C}}_{11}^{-1}\cdot\underline{\mathbf{M}}_{11}\cdot\underline{x}_{1,k} - \underline{\mathbf{Q}}_{22}^{\mathrm{T}}\cdot\underline{\mathbf{C}}_{22}^{-1}\cdot\underline{\mathbf{M}}_{22}\cdot\underline{x}_{2,k} \\
\underline{\mathbf{Q}}_{23}\cdot\underline{\mathbf{C}}_{22}^{-1}\cdot\underline{\mathbf{M}}_{22}\cdot\underline{x}_{2,k} - \underline{\mathbf{Q}}_{33}^{\mathrm{T}}\cdot\underline{\mathbf{C}}_{33}^{-1}\cdot\underline{\mathbf{M}}_{33}\cdot\underline{x}_{3,k}
\end{vmatrix} \tag{29}$$

Thus, the kinematic unknowns are determined from the static unknowns, solving the "mixed problem".

Sufficient but not necessary condition to solve the Eq. (29) is:

$$n_{xi} \geq n_{\lambda i} \tag{30}$$

where, n_{x_i} and n_{λ_i} are the variable freedom degrees numbers [5].

The corresponding eigenvalue is computed using the Rayleigh quotient.

$$\left(\omega^2\right)_{k+1} = \sum_{i=1}^{n} \frac{\underline{x}_{i,k+1}^{\mathrm{T}}\cdot\underline{\mathbf{M}}_{ii}\cdot\underline{x}_{i,k}}{\underline{x}_{i,k+1}^{\mathrm{T}}\cdot\underline{\mathbf{M}}_{ii}\cdot\underline{x}_{i,k+1}} \tag{31}$$

Being the mass sub-matrix $\mathbf{M}_{ii}$ positive definite matrices associated with each of the layers, it is ensured that the divisor of Eq. (31) is not zero.

Then, the resulting vector is normalized so that the new vector meets:

$$\sum_{i=1}^{n} \bar{\underline{x}}_{i,k+1}^{\mathrm{T}}\cdot\underline{\mathbf{M}}_{ii}\cdot\bar{\underline{x}}_{i,k+1} = 1 \tag{32}$$

The normalization keeps vector elements with similar values in each iteration. If not done, the element values increase and decrease in each step, and can cause numerical problems.

Checking of convergence is done by comparing two successive values of the eigenvalue.

$$\left\| \frac{\left(\omega^2\right)_{k+1} - \left(\omega^2\right)_k}{\left(\omega^2\right)_{k+1}} \right\| \leq tolerance \tag{33}$$

If the convergence criterion is not satisfied, a new iteration using as a test vector that is obtained by resolving Eq. (27) is started. The procedure is repeated until the convergence is set. As the number of iterations increases, eigenvalue and eigenvector tends to the lowest.

Assessment modes and frequencies above can be accomplished by introducing a shifting in the scale of eigenvalues, or establishing an orthogonal test vector orthogonal to the found eigenvectors

5. Numerical Results

From the presented model, a code in the software GNU Octave for the numerical analysis of free undamped vibration composite plates is implemented. The effects on the frequency of the anisotropic of the material, the thickness-to-side ratio and the number of layers are studied. Moreover, variation across the thickness of the transverse stresses associated with the fundamental mode is presented.

The plates have a rectangular geometry analyzed with dimensions a, b coincident with the x, y directions, respectively (Fig. 2). In all examples, they are modeled for symmetry reasons for the fundamental mode of vibration, only a quarter of the plate with a 6 × 6 uniform isoparametric quadrilateral elements with four-node linear interpolation mesh. The numerical evaluation of the integral is performed from the Gauss quadrature method, using 2 × 2 points membrane terms and flexure inertia while 1 × 1 points related to the shear.

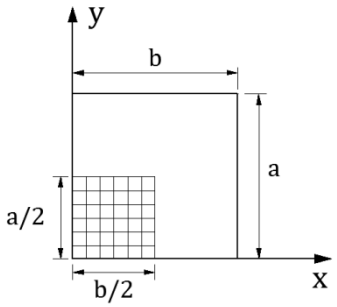

Fig. 2 Plate and mesh representation.

The boundary conditions used are:

$$\begin{aligned} (x,0): &\qquad w = u_{ox} = \beta_x = 0 \\ (0,y): &\qquad w = u_{oy} = \beta_y = 0 \\ (x,b/2): &\qquad u_{oy} = \beta_y = 0 \\ (a/2,y): &\qquad u_{ox} = \beta_x = 0 \end{aligned} \tag{34}$$

The mechanical elastic properties are:

$$\begin{aligned} &\frac{G_{23}}{E_2} = 0.60 \qquad \nu_{12} = 0.25 \\ &\frac{G_{12}}{E_2} = 0.50 \qquad \frac{G_{13}}{E_2} = 0.50 \end{aligned} \tag{35}$$

The effects on the natural frequencies of the number of layers as well as of the degree of orthotropy thereof are showed in Tables 1-4, where values in brackets indicate the number of layers of calculation. A square composite plate with a thickness/side ratio h/a = 0.20 is considered. The E_1/E_2 ratio and the number of layers vary. The results are compared with the solution of 3D elasticity [6], noting an excellent correlation. It follows that as the number of layers (i.e., the overall degree of anisotropy of the plate) is increased, so does the fundamental frequency. It is further noted that as the layers of calculation increases, the presented solution is refined. By enhancing the thickness discretization more realistically, shearing energy is computed assuming constant in each layer.

The effect of thickness/side ratio at the fundamental frequency is studied in Table 5. A laminated square plate $(0°/90°)_s$ with a E_1/E_2 = 40 ratio is analyzed. Each individual layer is discretized into three layers of calculation. The results are compared with those of other authors.

Table 1 Effect of the degree of orthotropy of each layer on the fundamental frequency of a simply supported squared plate with h/a = 0.20. Stacking sequence: (0°/90°).

	E_1/E_2 ratio				
	3	10	20	30	40
Present (2)	6.3350	7.0827	7.8000	8.3385	8.7610
Present (4)	6.2810	7.0322	6.7642	8.3092	8.7362
Present (6)	6.2672	7.0085	7.7197	8.2425	8.6482
Present (8)	6.2622	6.9990	7.7015	8.2150	8.6120
Present (10)	6.2597	6.9945	7.6925	8.2015	8.5940
Noor [6]	6.2577	6.9845	7.6745	8.1762	8.5625

Table 2 Effect of the degree of orthotropy of each layer on the fundamental frequency of a simply supported squared plate with h/a = 0.20. Stacking sequence: $(0°/90°)_2$.

	E_1/E_2 ratio				
	3	10	20	30	40
Present (4)	6.5562	8.1948	9.5107	10.313	10.862
Present (8)	6.5340	8.1382	9.4080	10.175	10.697
Present (12)	6.5297	8.1272	9.3872	10.147	10.662
Noor [6]	6.5455	8.1445	9.4055	10.165	10.680

Table 3 Effect of the degree of orthotropy of each layer on the fundamental frequency of a simply supported squared plate with h/a = 0.20. Stacking sequence: $(0°/90°)_3$.

	E_1/E_2 ratio				
	3	10	20	30	40
Present (6)	6.6002	8.4205	9.8697	10.746	11.338
Present (12)	6.5895	8.3918	9.8157	10.671	11.249
Noor [6]	6.6100	8.4142	9.8397	10.696	11.273

Table 4 Effect of the degree of orthotropy of each layer on the fundamental frequency of a simply supported squared plate with h/a = 0.20. Stacking sequence: $(0°/90°)_5$.

	E_1/E_2 ratio				
	3	10	20	30	40
Present (10)	6.6230	8.5400	10.065	10.986	11.610
Noor [6]	6.6457	8.5625	10.084	11.003	11.624

Table 5 Fundamental frequency for a simply supported squared plate with various h/a ratios (E_1/E_2 = 40).

h/a ratio	Desai et al. [7]	Matsunaga [8]	Present
0.50	5.315	5.3211	5.3462
0.20	10.682	10.6876	10.730
0.10	15.069	15.0721	15.160
0.05	17.636	17.6369	17.770
0.04	18.067	18.0557	18.198
0.02	18.670	18.6702	18.826
0.01	18.835	18.8352	18.995

Regarding the performance of the methodology of solving the problem of eigenvalues, the results were obtained with a relative error less than 1e-6 in a number of iterations alternating between 4 and 5, depending on the cases. Examples requiring more iteration cycle were related to a high E_1/E_2 ratio.

Finally, the behavior of the static variables is analyzed. Considered for h/a = 0.30 ratio , two square plates with a sequence of laminated (0°/90°) and $(0°/90°)_2$, and for h/a = 0.20 ratio, a square plate laminated with a scheme $(0°/90°)_5$. Variation along the thickness of the transversal stresses manners computed through Lagrangian multipliers is shown in Figs. 3-8. Obtained values are divided by their absolute maximum value. In all cases, the results obtained are similar to those found by the solution of the elasticity of Noor [6], the analytical solution of the global higher-order plate theory of Matsunaga [8], and tridimensional mixed finite element solution of Desai et al. [8].

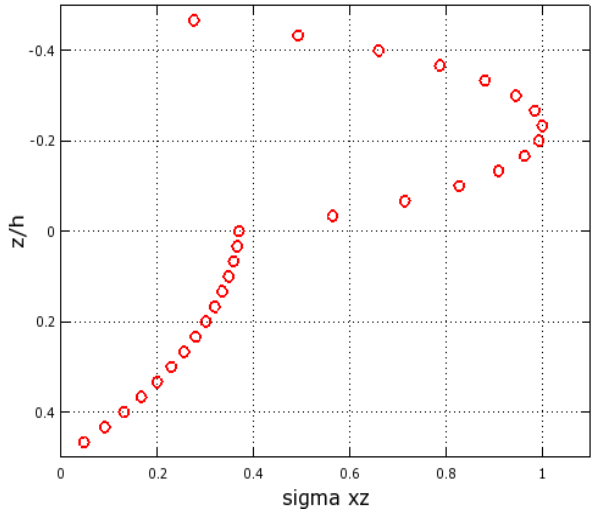

Fig. 3 Variation across the thickness of the normalized transverse shear stress $\bar{\sigma}_{xz}(0, b/2, \bar{z})$ for a simply supported squared plate with a stacking sequence (0º/90º).

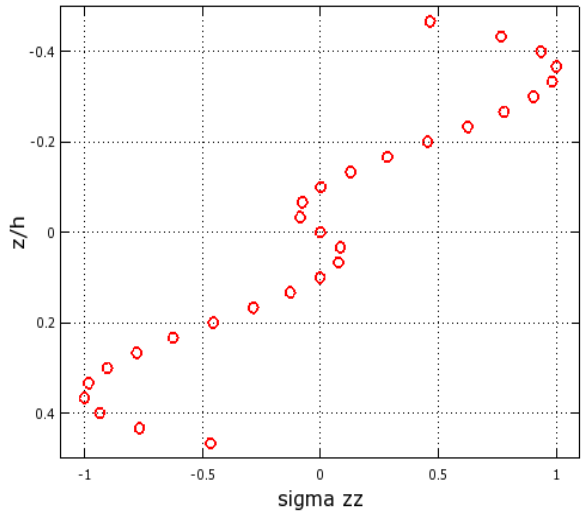

Fig. 4 Distribution along the thickness of the normalized transverse normal stress $\bar{\sigma}_{zz}(a/2, b/2, \bar{z})$ for a simply supported squared plate with a stacking sequence (0º/90º).

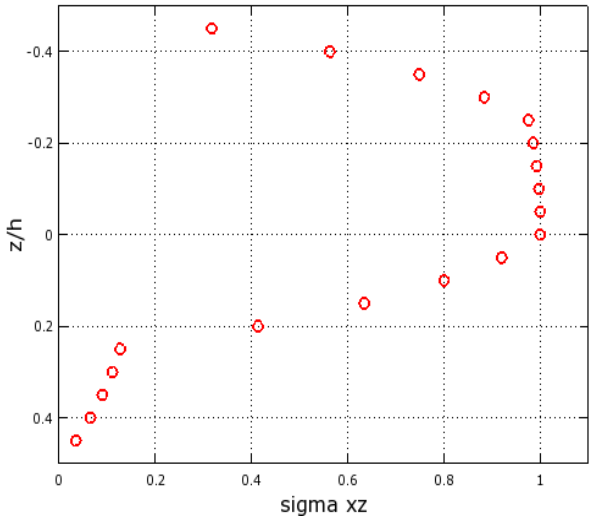

Fig. 5 Variation across the thickness of the normalized transverse shear stress $\bar{\sigma}_{xz}(0, b/2, \bar{z})$ for a simply supported squared plate with a stacking sequence $(0º/90º)_2$.

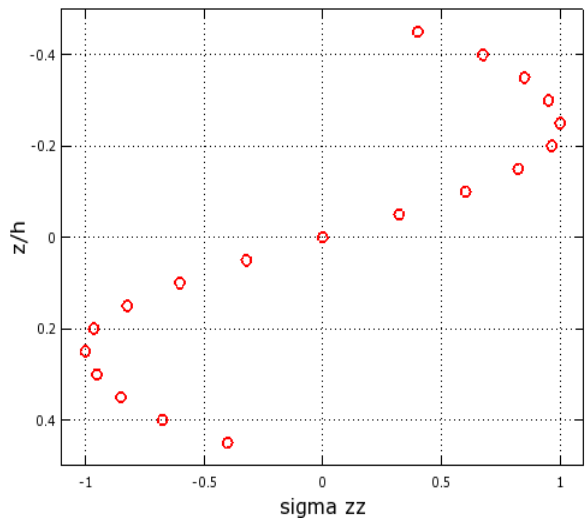

Fig. 6 Variation across the thickness of the normalized transverse shear stress $\bar{\sigma}_{zz}(a/2, b/2, \bar{z})$ for a simply supported squared plate with a stacking sequence $(0º/90º)_2$.

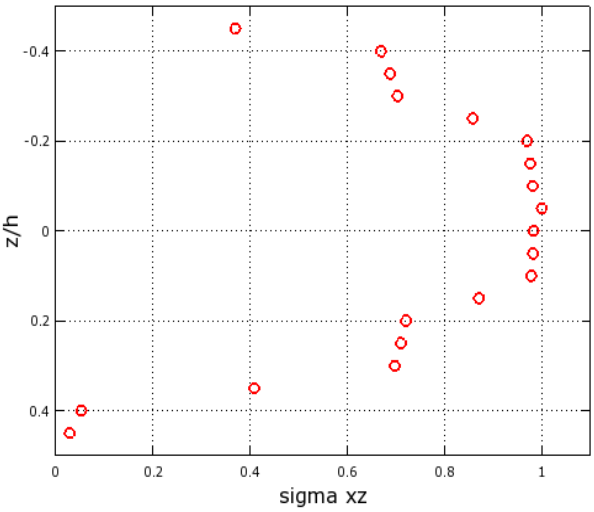

Fig. 7 Variation across the thickness of the normalized transverse shear stress $\bar{\sigma}_{xz}(0, b/2, \bar{z})$ for a simply supported squared plate with a stacking sequence $(0°/90°)_5$.

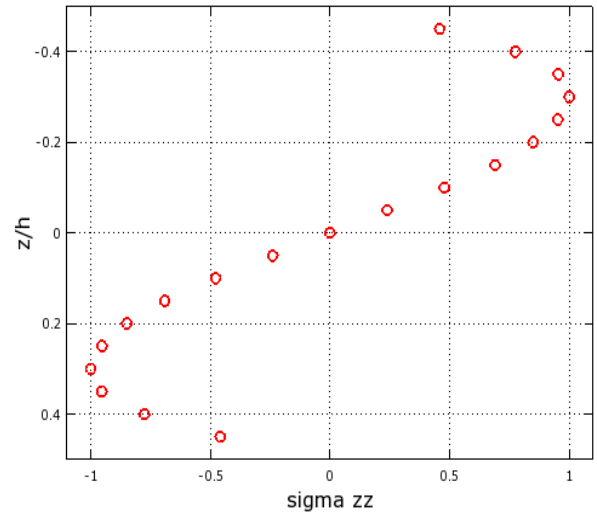

Fig. 8 Variation across the thickness of the normalized transverse shear stress $\bar{\sigma}_{zz}(a/2, b/2, \bar{z})$ for a simply supported squared plate with a stacking sequence $(0°/90°)_5$.

6. Conclusions

It presents a mixed finite element model to determine the modal characteristics of multilayered plates. The continuity of displacements as well as transverse stresses is assured across the thickness of the plate from the inclusion of Lagrange multipliers. The mixed formulation allows direct evaluation of transverse stresses without integrating the equilibrium equations involving loss of accuracy, resulting in a point of great interest in studying the behavior of composite laminates. A methodology based on the inverse iteration method to solve the eigenproblem was implemented, obtaining good results in a few iterations. The accuracy of the model is demonstrated along of several problems where the found results are similar to those available in the literature.

References

[1] Jones, R. M. 1999. *Mechanics of Composite Materials.* 2nd ed. United Kingdom: Taylor & Francis.

[2] Alliney, S., and Carnicer, R. S. 1992. "A Hybrid Finite Element Model for Multilayered Plates." *Computational Mechanics* 10 (5): 319-33.

[3] Reddy, J. R. 2003. *Mechanics of Composite Plates and Shells.* 2nd ed. United Kingdom: CRC Press.

[4] Chopra, A. K. 1995. *Dynamics of Structures: Theory and Applications to Earthquake Engineering.* New Jersey: Prentice Hall.

[5] Zienkiewicz, O. C., and Taylor, R. L. 2000. *The Finite Element Method: The Basis.* 5th ed. United Kingdom: Butterworth-Heinemann.

[6] Noor, A. K. 1973. "Free Vibration of Multilayered Composites Plates." *American Institute of Aeronautics and Astronautics Journal* 11 (7): 1038-9.

[7] Desai, Y. M., Ramtekkar, G. S., and Shah, A. H. 2003. "Dynamics Analysis of Laminated Composite Plates Using a Layer-Wise Mixed Finite Element Model." *Composite Structures* 59: 237-49.

[8] Matsunaga, H. 2000. "Vibration and Stability of Cross-Ply Laminated Composite Plates According to a Global Higher-Order Plate Theory." *Composite Structures* 48: 231-44.